*Exploration Geophysics (1998) **29**, 249-253*

# Magnetic permeability and electrical resistivity mapping with a multifrequency airborne EM system

**Haoping Huang**
**Douglas C. Fraser**
*Geoterrex-Dighem,*
*2270 Argentia Road, Unit 2,*
*Mississauga, Ontario,*
*Canada L5N 6A6.*

## ABSTRACT

The algorithms currently used to generate the apparent resistivity from helicopter EM data are not reliable in highly magnetic areas. This is because magnetic polarisation currents occur in addition to conduction currents, causing the computed resistivity to be erroneously high.

A new method for computing the apparent resistivity and apparent magnetic permeability has been developed for the magnetic conductive half-space. The inphase and quadrature responses at the lowest frequency are first used to estimate the apparent magnetic permeability. The apparent resistivity is then computed for all frequencies using the quadrature responses alone.

The EM response of magnetically permeable material is much greater for the inphase component than for the quadrature component. This means that the calculation of resistivity using the quadrature component at two frequencies is less subject to error from magnetic polarisation than if the inphase and quadrature components at a single frequency are used. The method allows the EM data to be portrayed as credible resistivity maps when magnetic polarisation currents occur in addition to conduction currents.

## INTRODUCTION

Apparent resistivity is typically derived from helicopter-borne EM data by using the pseudo-layer half-space model of Fraser (1978). This model yields the apparent resistivity and the apparent sensor-source distance directly from a transformation of the inphase and quadrature components. The EM bird altitude is not used. The pseudo-layer is merely an artifice to account for differences between the computed sensor-source distance and the measured bird altitude. The method used to calculate the apparent resistivity works well in non-magnetic areas. However it yields erroneous resistivities in highly magnetic areas because both inphase and quadrature components are affected by magnetic polarisation.

We have developed a method for computing the apparent magnetic permeability and the apparent resistivity of a magnetic conductive half-space. We use the inphase and quadrature components at the lowest frequency to estimate the apparent magnetic permeability at low induction number, and then use the quadrature from two adjacent frequencies to compute the apparent resistivity. The quadrature components are used from two frequencies, rather than the inphase and quadrature at a single frequency, to avoid the considerable impact that magnetic permeability has on the inphase component. The use of the expression *apparent resistivity* below refers specifically to the resistivity computed from the quadrature responses from two frequencies.

Unlike the inversion method of Zhang and Oldenburg (1997), the transform method described herein makes no assumptions as to the resistivity in the derivation of the apparent magnetic permeability.

## THEORY

For closely coupled transmitting and receiving coils, the ratio of secondary magnetic field intensity $H_s$ to primary magnetic field intensity $H_o$, at the receiving coil, can be approximated as (Fraser, 1972),

$$H_s/H_o = (s/h)^3 [M(\theta,\mu_r) + iN(\theta,\mu_r)] \quad . \qquad (1)$$

The measured inphase $I$ and quadrature $Q$ components may be represented as

$$I = (s/h)^3 M \qquad \text{and} \qquad Q = (s/h)^3 N \,, \qquad (2)$$

where the $I$ and $Q$ amplitudes are expressed in units of parts per million (ppm) of the primary magnetic field intensity $H_o$ at the receiving coil.

$M$ and $N$ respectively are the inphase and quadrature components of the response function $M + iN$, and portray the inphase and quadrature ppms scaled for variations in flying height $h$ and coil separation $s$.

$M$ and $N$ are functions of the dimensionless induction number $\theta = (\omega\sigma\mu h^2)^{1/2}$ and the relative magnetic permeability $\mu_r$, where $\sigma$ and $\mu$ are respectively the conductivity and permeability of the half-space, $\omega$ is the angular frequency of the EM system and $h$ is its height above the half-space. The relative magnetic permeability $\mu_r = \mu/\mu_o$, where $\mu_o$ is the permeability of free space.

Figure 1 shows $M$ and $N$ as functions of induction number $\theta$ for various values of $\mu_r$ for horizontal coplanar coils over a homogeneous half-space. The effect of a magnetic permeability $\mu > \mu_o$ is twofold. First, the permeability increases the value of the induction number $\theta$. Second, at very low induction number, the response function $M + iN$ becomes dominated by the magnetisation effect which is inphase with, and in the same direction as, the primary field. Thus, the inphase component $M$ of the response function becomes frequency-independent (signed negative by convention) and the quadrature component $N$ tends to zero as the induction number $\theta$ approaches zero. At the other extreme, as $\theta \to \infty$, the response function $M + iN$ becomes dominated by the conductive effect which is inphase with, and in the opposing direction of, the primary field. Thus, the inphase component $M$ of the response function becomes frequency-independent (signed positive) and the quadrature component $N$ tends to zero as the induction number $\theta$ approaches infinity. At high induction numbers, the

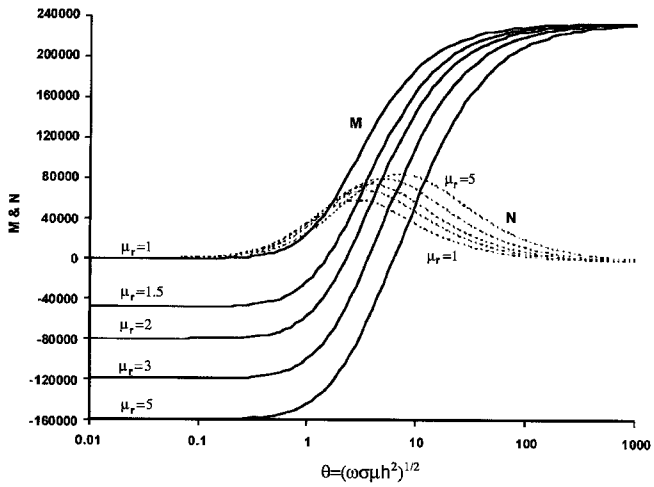


**Figure 1. Inphase $M$ and quadrature $N$ components of the response function of a homogeneous half-space vs. the induction number $\theta$ for various values of the relative magnetic permeability $\mu_r$, for horizontal coplanar coils.**

permeability become irrelevant and so all curves in Figure 1 converge to that for $\mu_r = 1$ as $\theta \rightarrow \infty$. For mid-range induction numbers, the magnetisation effect and conductive effect are mixed and the response function becomes frequency dependent.

## Determination of the apparent relative permeability

We obtain the relative magnetic permeability from the observed EM data at the lowest available induction number. Both the inphase and quadrature ppms are used. While the method is applicable in the presence of conduction currents, we use EM data from the lowest frequency to ensure that the induction number $\theta$ is as low as possible to maximise the ratio of magnetic response to conductive response.

The inphase $M$ of the response function is plotted against relative magnetic permeability $\mu_r$ in Figure 2a for several low to moderate induction numbers $\theta$. If the condition $\theta < 0.1$ is satisfied at the lowest operating frequency, as evidenced by the lack of a measured quadrature response, $\mu_r$ can be determined directly from the inphase component $M$ using the curve for $\theta < 0.1$ in Figure 2a. In this case, $M$ is first obtained from equation (2) on the assumption that the bird height from the altimeter can be used in place of the unknown sensor-source distance $h$. However, if conduction currents exist as evidenced by the presence of a measured quadrature response, the induction number $\theta$ at the lowest frequency has to be estimated first. We can see from Figure 1 that the quadrature component of the response function for $\theta < 4$ is fairly independent of $\mu_r$, and depends mainly upon $\theta$. In this case, the quadrature component $N$ may be used to estimate the induction number from Figure 2b, where $N$ is obtained first from equation (2) assuming $h$ is derived from the altimeter. The error bars in Figure 2b show the uncertainty arising from the fact that the quadrature component $N$ is not totally independent of the relative magnetic permeability. These error bars reflect the variation in the quadrature values for different $\mu_r$ as shown in Figure 1.

The relative magnetic permeability may be obtained from the inphase component $M$ using the curve in Figure 2a for the same induction number as obtained above from Figure 2b. If the earth is a true homogeneous magnetic half-space, the relative magnetic permeability $\mu_r$ obtained in this way would be the true relative permeability. Otherwise, it would be the apparent relative permeability.

The relative magnetic permeability $\mu_r$, obtained as a by-product of resistivity mapping, can be transformed into the apparent susceptibility $\kappa = \mu_r - 1$ in SI units for purposes of map display.

## Determination of the apparent resistivity

Since the relative magnetic permeability $\mu_r$ is an independent variable in equation (1), the quadrature ratio $Q_L/Q_H$ from two adjacent frequencies and the normalised amplitude $A_{QQ} = (Q_L + Q_H)(h/s)^3 = N_L + N_H$ can be plotted against the induction number $\theta_L$ for various values of $\mu_r$ (Figure 3). We use the symbol $\theta_L$ for the induction number to indicate that the low frequency $f_L$ must be used to solve for the resistivity given the induction number from Figure 3a. The frequency ratio $f_H/f_L$ for these curves is fixed at 8 to match a common frequency separation for DIGHEM helicopter EM systems. If $\mu_r$ has been determined from the lowest frequency as per the above section, the induction numbers $\theta_L$ can be obtained for all pairs of adjacent frequencies using the appropriate curve in Figure 3a. Then, the normalised amplitudes $A_{QQ}$ are determined from Figure 3b, given the induction numbers $\theta_L$ for all pairs of adjacent frequencies.

The apparent height $h_a$ is then calculated from the two quadrature ppms $Q_L$ and $Q_H$ and from the amplitude function $A_{QQ}$ from Figure 3b, i.e.,

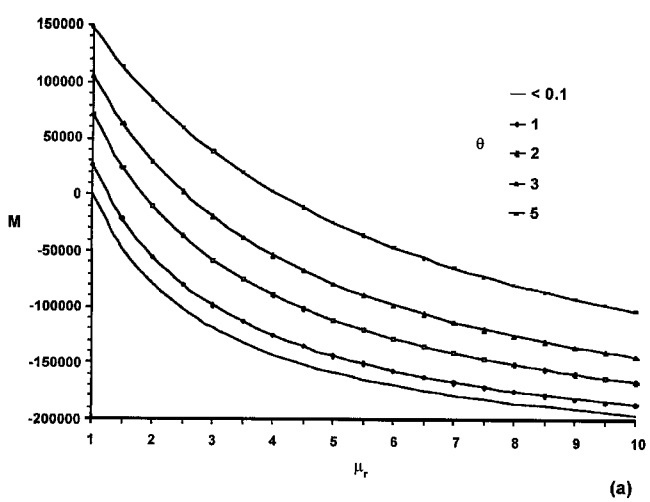


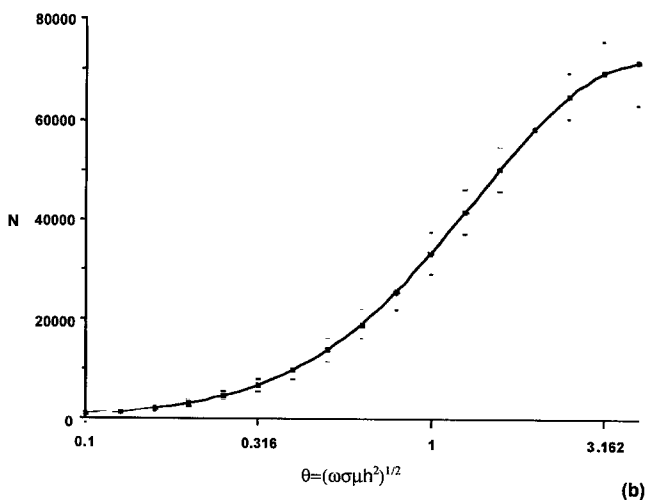


**Figure 2. (a) The inphase $M$ of the response function vs. relative magnetic permeability $\mu_r$ for low and moderate induction numbers $\theta$. (b) The quadrature $N$ of the response function versus low induction number $\theta$.**

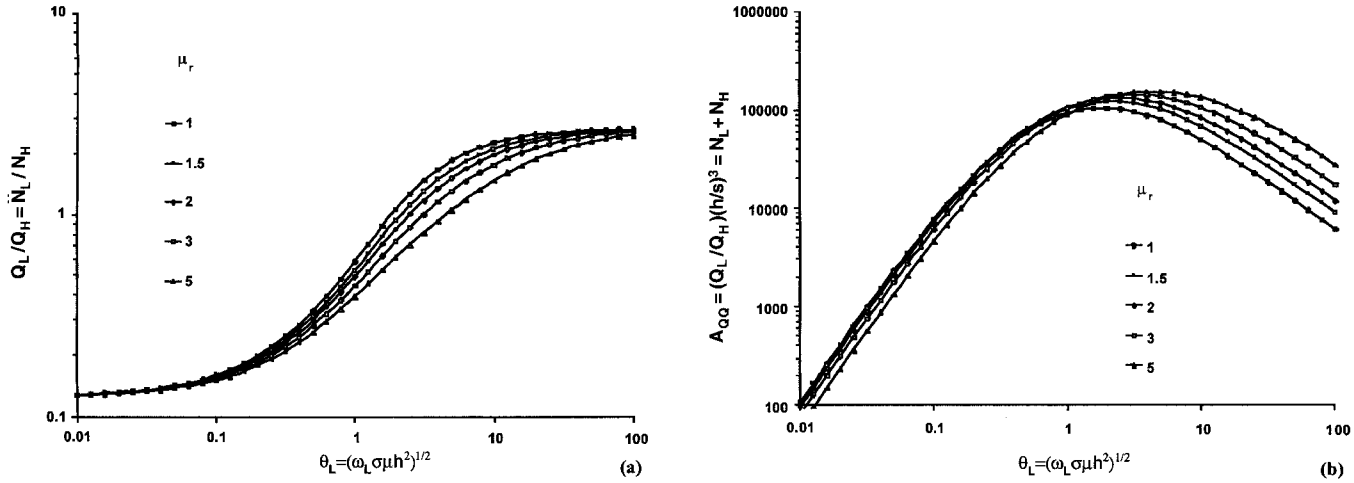


**Figure 3. (a) The ratio $Q_L/Q_H$ and (b) the normalised amplitude $A_{QQ} = (Q_L + Q_H)(h/s)^3 = N_L + N_H$ as a function of the induction number $\theta$ for various values of the relative permeability $\mu_r$ and a frequency ratio of 8.**

$$h_a = s\,[A_{QQ}/(Q_L+Q_H)]^{1/3}, \quad (3)$$

where $s$ is the transmitting-receiving coil separation.

The apparent thickness $t_a$ of the pseudo-layer is given as

$$t_a = h_a - a \quad (4)$$

where $a$ is the EM bird height obtained from the altimeter.

The resistivity $\rho$, which is the reciprocal of the conductivity $\sigma$, is then calculated from the induction number $\theta = \theta_L$ at the low frequency as

$$\rho_a = 2\pi\mu f_L\,(h_a/\theta)^2, \quad (5)$$

where $\rho_a$ is the apparent resistivity of the pseudo-layer model, and the permeability $\mu$ is the apparent permeability determined above.

Equations (3), (4) and (5), along with Figure 3, can be used to convert the observed quadrature responses of a pair of frequencies, separated by a factor of 8 (for example, as per the DIGHEM system) to the apparent thickness (of the pseudo-layer) and the apparent resistivity (of the underlying half-space) using the pseudo-layer half-space model. If the earth is truly homogeneous, the resistivity obtained from equation (5) is the true resistivity $\rho$. Otherwise, it would be the apparent resistivity $\rho_a$.

## MODEL DATA TESTS

Figure 4 shows how the apparent resistivity behaves for a *non-magnetic* two-layer model where the thickness of the upper layer $t_1$ increases from left to right. The upper-layer resistivity of 50 ohm-m and the basement resistivity of 500 ohm-m simulates moderately conductive overburden on a relatively resistive basement.

Figure 5 shows the apparent resistivities for the same model as in Figure 4, but with various permeabilities, although the permeability is uniform for the two layers of the model. Such a model could simulate conductive cover over bedrock where the cover was produced by weathering or erosion which neither attenuated nor concentrated the magnetite.

Each panel of Figure 5 has one apparent resistivity curve in common with those of Figure 4, these being the curves for the relative magnetic permeability $\mu_r = 1$. The apparent resistivity curves for several permeabilities, for the 7200Hz-56kHz frequency pair and for 900-7200Hz, are respectively shown in Figures 5a and 5b.

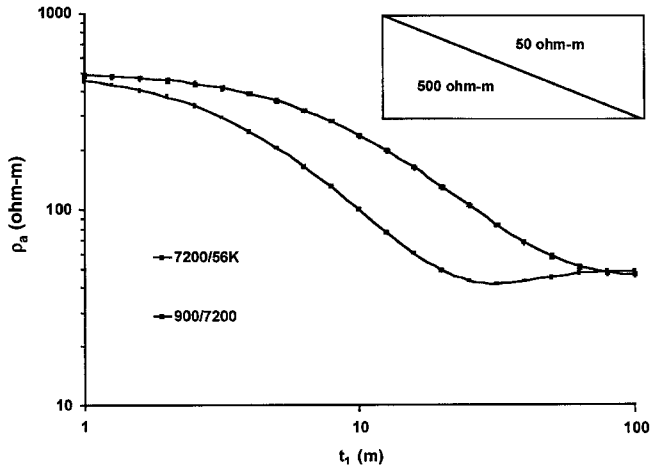


**Figure 4. The apparent resistivity $\rho_a$ obtained from the quadrature ppms from 7200 Hz and 56 kHz, and from 900 and 7200 Hz, for a two-layer model with a relative permeability $\mu_r$ of 1. While the thickness of the upper layer varies, the resistivities of the upper layer and the basement are respectively fixed at 50 and 500 ohm-m.**

In generating the panels of Figure 5, the forward solutions yielded the inphase and quadrature ppms for the various frequencies. The permeability was first determined from the 900 Hz data. The permeability was then used along with the quadrature ppms to obtain the apparent resistivity.

The curves of Figure 5 illustrate that the apparent resistivities are impacted somewhat by the permeability. Thus, when $\mu_r > 1$, the transform yields permeability-dependent values for the apparent resistivities even when the correct permeability is used in the transformation to the half-space model. The effect of the permeability on the apparent resistivity is generally not serious for those relative magnetic permeabilities which are usually encountered in practice, i.e., $\mu_r < 2$.

The magnetic two-layer cases studied above had the same permeability for each of the two layers. In our testing of magnetic-resistivity half-space transform methods, we have also varied the permeability of the layers independently which, of course, leads to many more combinations of parameters. Figure 6 presents one such example. This is a repeat of Figure 5 but with the upper layer being non-magnetic. Such a model simulates non-magnetic conductive cover over relatively resistive magnetic bedrock.

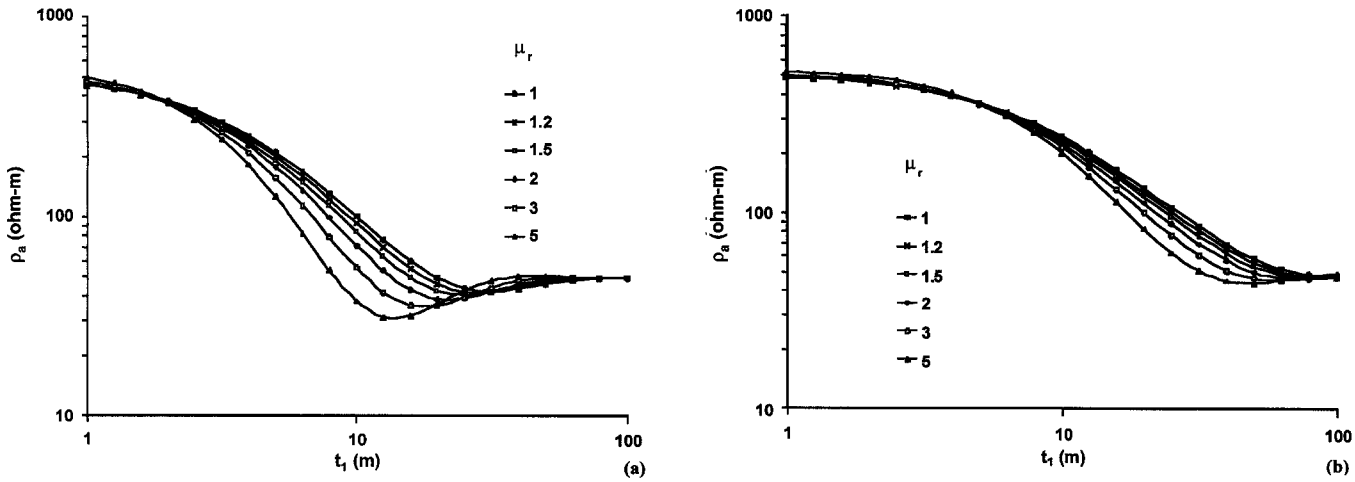


Figure 5. The apparent resistivity is shown for several permeabilities for (a) 7200 Hz and 56 kHz and (b) for 900 Hz and 7200 Hz, for the same model as Figure 4. The two-layer model has an upper layer resistivity of 50 ohm-m, a lower-layer resistivity of 500 ohm-m, and has a variable thickness of the upper layer as shown on the x-axis.

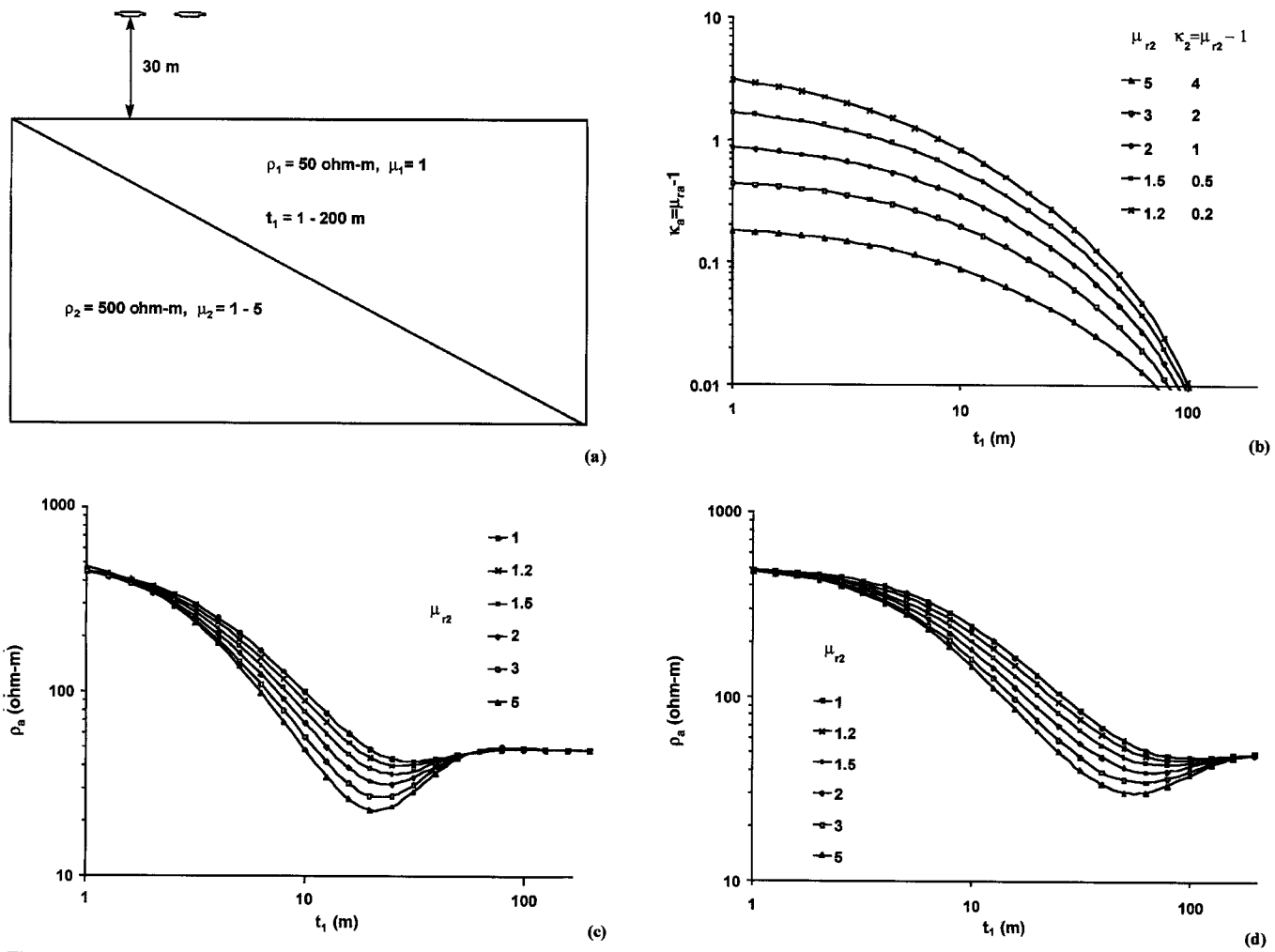


Figure 6. (a) The two layer model has a non-magnetic upper layer resistivity of 50 ohm-m, a variably magnetic lower-layer resistivity of 500 ohm-m, and a variable thickness of the upper layer as shown on the x-axis. (b) The apparent magnetic susceptibilities $\kappa$ are calculated from the 900 Hz EM data. The apparent resistivities are shown for several lower layer permeabilities for (c) 7200 Hz and 56 kHz and for (d) 900 and 7200 Hz.

The model shown in Figure 6a comprises a conductive upper layer of 50 ohm-m over a 500 ohm-m basal layer. There are two variables, comprising the thickness $t_1$ of the upper layer, which increases continuously to the right, and the relative magnetic permeability $\mu_r$ of the lower layer which varies discretely from 1 to 5.

Figure 6b shows the apparent susceptibility $\kappa = \mu_r - 1$ computed from the 900 Hz data. The apparent magnetic susceptibility is shown, rather than the apparent relative permeability, to provide a sensitivity to the display for the very small apparent permeability values which result when the non-magnetic cover exceeds 30 m in thickness. When

the cover is thin (e.g., 1 m), the computed susceptibility is very close to the true susceptibility of the lower layer. The computed values of the relative magnetic permeability were used along with the quadrature ppms to compute the apparent resistivities of Figures 6c and 6d.

## DISCUSSION

Some caution is required in the use of the two-frequency quadrature algorithm for calculating apparent resistivity. It may be misleading in areas yielding a high induction number, with the apparent resistivities being outside the range of the true resistivities (e.g., note the undershoot in the apparent resistivities in Figures 4, 5a, 6c and 6d). In particular, the algorithm should be avoided when using high frequencies in conductive areas. This usually is not a serious limitation, bearing in mind that the primary purpose of the quadrature resistivity algorithm is to be employed in highly magnetised areas and these in practice tend to be resistive. In contrast, in highly conductive areas, any magnetic polarisation currents which may exist are overwhelmed by the conduction currents, and so the resistivity may be calculated directly from the inphase and quadrature ppms without consideration of magnetic permeability.

The above noted undershoot occurrences are related to the skin depth and the depth to the two-layer interface. This raises the issue that the two frequencies used to compute the resistivity actually sample the earth to different depths and, hence, see different geology to some extent. This does not seem to be a serious issue in practice. This does, however, highlight the reason why the magnetic permeability obtained from magnetometer data should not be used as input to a resistivity algorithm. The volume of ground sampled by the inducing field of the earth's magnetic field and by the transmitting coil are so vastly different that they tend to yield quite different values for the apparent magnetic permeability.

## CONCLUSIONS

The apparent permeability and apparent resistivity may be computed using a permeable conductive half-space model using a technique developed for closely-coupled helicopter-borne electromagnetic systems. The permeable conductive half-space model uses the lowest available frequency to estimate the apparent magnetic permeability. This is followed by the computation of the apparent resistivity from the quadrature EM data at two frequencies, for each pair of adjacent frequencies of a multi-frequency system.

The resistivity algorithm may exhibit undershoots or overshoots in conductive areas for high frequencies, so a degree of caution should be exercised when applying it.

The permeable conductive half-space method expands the use of half-space models for resistivity mapping in magnetic terrains.

## REFERENCES

Fraser, D.C., 1972, A new multicoil aerial electromagnetic prospecting system: Geophysics, **27**, 518-537.

Fraser, D.C., 1978, Resistivity mapping with an airborne multicoil electromagnetic system: Geophysics, **43**, 144-172.

Zhang, Z., and Oldenburg, W., 1997, Recovering magnetic susceptibility from electromagnetic data over a one-dimensional earth: Geophys. J. Int. **130**, 422-434.